Journal of Statistical Physics, Vol. 121, Nos. 1/2, October 2005 (© 2005)
DOI: 10.1007/s10955-005-8413-z

A Lattice Boltzmann Kinetic Model for Microflow and Heat Transfer

C. Shu,[1] X. D. Niu,[1] and Y. T. Chew[1]

Received October 12, 2004; accepted July 22, 2005

In this paper, we propose a lattice Boltzmann BGK model for simulation of micro flows with heat transfer based on kinetic theory and the thermal lattice Boltzmann method (He *et al.*, *J. Comp. Phys.* **146**:282, 1998). The relaxation times are redefined in terms of the Knudsen number and a diffuse scattering boundary condition (DSBC) is adopted to consider the velocity slip and temperature jump at wall boundaries. To check validity and potential of the present model in modelling the micro flows, two two-dimensional micro flows including thermal Couette flow and thermal developing channel flow are simulated and numerical results obtained compare well with previous studies of the direct simulation Monte Carlo (DSMC), molecular dynamics (MD) approaches and the Maxwell theoretical analysis.

KEY WORDS: Lattice Boltzmann; micro thermal flow.

1. INTRODUCTION

As the development of micro electromechanical systems (MEMS), the flow and heat transfer in micro devices have become an area that receives a significant attention.[1–4] The mechanism of the microscopic flow and heat transfer is quite different from that of macroscopic counterparts because the characteristic length of the flow H is of comparable order of magnitude of the mean free path λ and the inter-molecular interactions are manifested. The microscopic flows are usually characterized by a dimensionless parameter–the Knudsen number $Kn = \frac{\lambda}{H}$. Theoretically, when $Kn > 0.01$, traditional hydrodynamic descriptions such as the Navier–Stokes (NS)

[1]Department of Mechanical Engineering, National University of Singapore, 10 Kent Ridge Crescent, Singapore 119260; e-mail: mpeshuc@nus.edu.sg

equations and Fourier heat conduction equation are invalid and the solvers of the full Boltzmann equation (BE)[5–7] and the particle-based methods such as molecular dynamics (MD)[8] and the direct simulation Monto Carlo (DSMC)[9] are often used for numerical studies. However, the computational effort of the MD and the DSMC is usually huge with the use of most powerful supercomputer and the schemes used for solving the full BE are complicated because it requires the integration of a six-independent-variables function.

Recently, the lattice Boltzmann method (LBM) has received a considerable attention by fluid dynamic researchers.[10–14] The guiding principle of the LBM is to construct a dynamic system on a regular lattice involving a number of the single-particle distribution functions of fictitious particles on the links of the lattice. The particles then evolve in a discrete time according to laws retaining the basic fluid principles of mass, moment and energy conservation. Unlike the MD and DSMC methods, the number of particles distributed in the computational field in the LBM is not related to the number of molecules. Therefore, the LBM is intuitively more computationally efficient than the MD and DSMC methods. Furthermore, since the LBM solver is based on a simple BGK collision approximation,[15] one avoids solving the complicated full BE. On the other hand, the LBM is intrinsically kinetic because the BGK collision approximation essentially represents the physics of molecular interactions and the equilibrium distribution function in it can be considered as an effective equilibrium of the molecular motions. Hence it has a strong theoretical foundation to be taken as an alternative to model the microscopic fluid dynamic problems.

In this paper, we present a lattice Boltzmann BGK model for simulating the micro flow and heat transfer. Our model is based on the classic kinetic theory[16] and the thermal lattice Boltzmann method (TLBM).[17] In the TLBM, the macroscopic velocity field and temperature field are simulated by the density distribution function and a new internal energy density distribution function, respectively. The difference of the present model with the TLBM is that we redefine the relaxation times in terms of the Knudsen number based on the kinetic theory,[16] and the LBM theory.[13–17] On the other hand, in consistence of the kinetic theory, a diffuse-scattering boundary condition (DSBC) for the LBM is presented so that the particle–solid interactions manifested in the micro level are reflected kinetically and the velocity slips and temperature jumps at walls are captured correctly.

To show the validity of the present lattice Boltzmann BGK model in simulation of the micro flows with heat transfer, a theoretical analysis of the DSBC for a simple thermal flow is presented, and a two-dimensional

(2D) thermal Couette flow and a developing thermal microchannel flow are studied using the Taylor series expansion and least square-based LBM (TLLBM).[18] The TLLBM has been proven to be an efficient and accurate solver for simulating the continuum flows with irregular grids.[19,20] The results obtained are compared with theoretical solutions and computation results.

2. THERMAL LATTICE BOLTZMANN MODEL

The thermal lattice Boltzmann equation with BGK model[17] can be written as

$$\bar{f}_\alpha(\vec{x}+\vec{e}_\alpha\delta_t, t+\delta_t) = \bar{f}_\alpha(\vec{x}, t) + \frac{\delta_t}{\tau_f + 0.5\delta_t}(f_\alpha^{\mathrm{eq}}(\vec{x}, t) - \bar{f}_\alpha(\vec{x}, t)), \tag{1}$$

$$\begin{aligned}\bar{g}_\alpha(\vec{x}+\vec{e}_\alpha\delta_t, t+\delta_t) = {} & \bar{g}_\alpha(\vec{x}, t) + \frac{\delta_t}{\tau_g + 0.5\delta_t}(g_\alpha^{\mathrm{eq}}(\vec{x}, t) - \bar{g}_\alpha(\vec{x}, t)) \\ & - \frac{\tau_g \delta_t}{\tau_g + 0.5\delta_t} f_\alpha(\vec{x}, t) h_\alpha(\vec{x}, t),\end{aligned} \tag{2}$$

where $\bar{f}_\alpha = f_\alpha - \frac{\delta_t}{2\tau_f}(f_\alpha^{\mathrm{eq}} - f_\alpha)$, $\bar{g}_\alpha = g_\alpha - \frac{\delta_t}{2\tau_g}(g_\alpha^{\mathrm{eq}} - g_\alpha) + \frac{\delta_t}{2} f_\alpha h_\alpha$ and $h_\alpha = (\vec{e}_\alpha - \vec{u}) \cdot [-\nabla(\frac{P}{\rho}) + \frac{1}{\rho}\nabla \cdot \Pi + (\vec{e}_\alpha - \vec{u}) \cdot \nabla \vec{u}]$; f_α and g_α are the density and internal energy distribution functions, respectively, and $g_\alpha = \frac{(\vec{e}_\alpha - \vec{u})^2}{2} f_\alpha$; f_α^{eq} and g_α^{eq} are their corresponding equilibrium functions; τ_f and τ_g are the relaxation times of the hydrodynamic and thermodynamic fields, respectively; $\vec{e}_\alpha$ is the lattice velocity, α is the lattice direction, δ_t is the time interval. The macroscopic density ρ, velocity $\vec{u}$, internal energy ε and pressure P can be computed by the conservation laws of mass, momentum, energy and the equation of state,

$$\rho = \sum_\alpha \bar{f}_\alpha, \quad \rho\vec{u} = \sum_\alpha \bar{f}_\alpha \vec{e}_\alpha; \quad \rho\varepsilon = \sum_\alpha \bar{g}_\alpha - \frac{\delta_t}{2}\sum_\alpha \bar{f}_\alpha h_\alpha; \quad P = \frac{2}{D}\rho\varepsilon, \tag{3}$$

where $\varepsilon = DRT/2$, T is the temperature and D is the dimension. In this work, we only consider a two-dimensional ($2D$) problem as an example. The equilibrium functions f_α^{eq} and g_α^{eq} with the $2D$ 9-bit discrete velocity (D2Q9) mode[12,17] are written as

$$f_\alpha^{\mathrm{eq}} = w_\alpha \rho \left[1 + \frac{3\vec{e}_\alpha \cdot \vec{u}}{c^2} + \frac{9(\vec{e}_\alpha \cdot \vec{u})^2}{2c^4} - \frac{3\vec{u}_\alpha^2}{2c^2}\right], \tag{4}$$

$$g_\alpha^{\mathrm{eq}} = w_\alpha \rho \varepsilon \left[\frac{2(\vec{e}_\alpha^2 - \vec{u}^2)}{2c^2} + 3\left(\frac{3\vec{e}_\alpha^2}{2c^2} - 1 \right) \frac{\vec{e}_\alpha \cdot \vec{u}}{c^2} + \frac{9(\vec{e}_\alpha \cdot \vec{u})^2}{2c^4} \right], \tag{5}$$

where $c = \sqrt{3RT_0}$ and T_0 is the average temperature.

3. THERMAL LBM FOR MICRO FLOWS WITH HEAT TRANSFER

Theoretically, the lattice Boltzmann BGK model provides a better framework to simulate the microscopic flows. Although the BGK model seems to describe only weak departures from local equilibriums, it has long been recognized[21] that such an approximation works well beyond its theoretical limits as long as the relaxation time can be made to capture the relevant physics.

3.1. Redefinition of Relaxation Times

In the Kinetic theory and the conventional lattice BE with BGK model, the relaxation time τ_f and τ_g are linked to the viscosity and thermal conductivity of fluid in the way that the correct hydrodynamics are described.[5,13,16,17,22] However, to model the microscopic hydrodynamics, the Knudsen effects should be considered.

From the kinetic theory,[5,16] we know that the collision frequency in the BGK model can be written as P/μ for hydrodynamic field or $2P/5R\kappa$ for thermodynamic field, where μ and κ are the viscosity and thermal conductivity of fluid, respectively. This implies that τ_f and τ_g can be written as

$$\tau_f = \frac{\mu}{P} = \frac{\mu}{\rho c_s^2}, \tag{6}$$

$$\tau_g = \frac{\mu}{\mathrm{Pr}\rho c_s^2}, \tag{7}$$

where c_s is the sound speed, Pr $(= \mu c_p/\kappa)$ is the Prandtl number, $c_p (= \gamma R/(\gamma - 1))$ is specific heat capacity and γ (=5/3 for a monatomic ideal gas and 7/5 for a diatomic gas) is the heat capacity ratio of gas.

According to kinetic theory,[5,16,23] the Knudsen number can be written as

$$Kn = \sqrt{\frac{\pi\gamma}{2}} \frac{Ma}{Re}, \tag{8}$$

where $Re = \rho U_\infty H/\mu$ is the Reynolds number and $Ma = U_\infty/c_s$ is the Mach number. For the D2Q9 model, c_s is taken as $c/\sqrt{3}$ and c is usually chosen as 1. Hence by combining Eqs. (6)–(8) we have

$$\tau_f = \sqrt{\frac{6}{\pi\gamma}} H \cdot Kn \approx H \cdot Kn, \tag{9}$$

$$\tau_g = \frac{H \cdot Kn}{\mathrm{Pr}}. \tag{10}$$

Equations (9) and (10) link the relaxation times in the LBM to the Knudsen number. These relations are critical for the micro flow simulation.

3.2. Diffuse Scattering Boundary Condition

The boundary condition is an important issue for the LBM and it has been well discussed by different authors for microfluidic systems[24–26] and for macroscopic flows.[27,28] In this work, a DBSC for the LBM to model micro flows is derived following the well-known Maxwell hypothesis[29] to capture the correct velocity slip and temperature jump at the wall.

Theoretically, the particle–solid interactions should be adequately addressed when the particles impinge and emerge at solid wall surfaces, and this issue should be traced to the kinetic theory. According to the gas–surface interaction law of the kinetic theory,[16,23,29] a general boundary condition reads

$$|(\vec{\xi} - \vec{u_w}) \cdot \vec{n}| f(\vec{\xi}) = \int_{(\vec{\xi}' - \vec{u_w}) \cdot \vec{n} < 0} |(\vec{\xi}' - \vec{u_w}) \cdot \vec{n}| \Re(\vec{\xi}' \longrightarrow \vec{\xi}) f(\vec{\xi}') d\vec{\xi}', \tag{11}$$

where $\vec{\xi}'$ and $\vec{\xi}$ are molecular velocities of the incident and reflected particles, respectively, $\vec{n}$ is the inward unit normal vector of the wall and w indicates the wall boundary. $\Re(\vec{\xi}' \longrightarrow \vec{\xi})$ is the scattering kernel stratifying the normalization condition

$$\int_{(\vec{\xi} - \vec{u_w}) \cdot \vec{n} > 0} \Re(\vec{\xi}' \longrightarrow \vec{\xi}) d\vec{\xi} = 1 \quad (\vec{\xi}' - \vec{u_w}) \cdot \vec{n} < 0 \tag{12}$$

and the reciprocity relation

$$|(\vec{\xi}' - \vec{u_w}) \cdot \vec{n}| f_w^{\mathrm{eq}}(\vec{\xi}') \Re(\vec{\xi}' \longrightarrow \vec{\xi}) = |(\vec{\xi} - \vec{u_w}) \cdot \vec{n}| f_w^{\mathrm{eq}}(\vec{\xi}) \Re(-\vec{\xi} \longrightarrow -\vec{\xi}') \tag{13}$$

if the surface is staying in local equilibrium at the wall temperature T_w. There are some special models for the scattering kernel $\Re(\vec{\xi}' \longrightarrow \vec{\xi})$.[16,23] The most well known one is Maxwell's diffuse scattering model,[16] which has the following form

$$\Re(\vec{\xi}' \longrightarrow \vec{\xi}) = \frac{1}{\rho_w RT_w (2\pi RT_w)^{-\frac{1}{2}}} [(\vec{\xi} - \vec{u_w}) \cdot \vec{n}] f^{\mathrm{eq}}(\vec{\xi})|_{\vec{u}=\vec{u_w}}, \tag{14}$$

where f^{eq} is the Maxwell distribution function. Physically, the Maxwell diffuse scattering boundary condition assumes that a particle coming to the solid wall forgets all information on its state before the collision occurs on the wall, and then leaves the wall with the Maxwellian distribution function.

Since the distribution function f_α in the LBM is actually the projection of the continuous distribution function $f(\vec{\xi})$ in a finite dimensional velocity space, and its equilibrium f_α^{eq} is simplified from the Maxwellian equilibrium $f^{\mathrm{eq}}(\vec{\xi})$ using truncated Taylor series expansion,[13,17] Eqs. (11) and (14) naturally leads to the following DSBC for the LBM:

$$|(\vec{e}_\alpha - \vec{u_w}) \cdot \vec{n}| f_\alpha = \sum_{(\vec{e}_{\alpha'} - \vec{u_w}) \cdot \vec{n} < 0} |(\vec{e}_{\alpha'} - \vec{u_w}) \cdot \vec{n}| \Re_f (\vec{e}_{\alpha'} \longrightarrow \vec{e}_\alpha) f_{\alpha'}, \tag{15}$$

where $\Re_f(\vec{e}_{\alpha'} \longrightarrow \vec{e}_\alpha) = \frac{A_N}{\rho_w}[(\vec{e}_\alpha - \vec{u_w}) \cdot \vec{n}] f_\alpha^{\mathrm{eq}}$ with α' and α are directions of the incident and reflected particles, respectively. A_N is a normalized coefficient and can be obtained by satisfying Eqs. (12) and (13), which guarantees no normal flow through the wall ($\vec{u} \cdot \vec{n} = \sum_\alpha f_\alpha (\vec{e}_\alpha \cdot \vec{n}) = 0$). This coefficient is also dependent on the velocity model used in the LBM. Equation (15) is just a velocity boundary condition in the LBM simulation. It should be indicated that similar expressions to Eq. (15) were also postulated by Gatignol[30] for discrete velocity models of the kinetic theory and recently by Ansumali and Karlin[31] for the LBM.

In order to get the thermal boundary condition for the LBM, we should bear in mind that the normal part of the energy flux ($\int \frac{\vec{\xi}^2}{2} \vec{\xi} f \, d\vec{\xi}$) is continuous at the wall. Using the defination of g_α, we can obtain the following thermal DSBC for the present LBM analogically from Eq. (11)

$$|(\vec{e}_\alpha - \vec{u_w}) \cdot \vec{n}| g_\alpha = \sum_{(\vec{e}_{\alpha'} - \vec{u_w}) \cdot \vec{n} < 0} |(\vec{e}_{\alpha'} - \vec{u_w}) \cdot \vec{n}| \Re_g (\vec{e}_{\alpha'} \longrightarrow \vec{e}_\alpha) g_{\alpha'}, \tag{16}$$

where $\Re_g(\vec{e}_{\alpha'} \longrightarrow \vec{e}_\alpha) = \frac{B_N}{\rho_w \varepsilon}[(\vec{e}_\alpha - \vec{u_w}) \cdot \vec{n}] g_\alpha^{\mathrm{eq}}$ and B_N is a normalized coefficient and can be obtained by $\sum_\alpha g_\alpha (\vec{e}_\alpha \cdot \vec{n}) = 0$.

4. THEORETICAL ANALYSIS OF THE DSBC

To show whether the proposed DSBC can correctly capture the velocity slips and the temperature jumps on the wall, theoretical analyses based on a 2D constant density flow along an infinite plate with a constant velocity U_0 and a constant temperature T_0 (therefore the internal energy $\varepsilon_0 = RT_0$) are carried out in this part. The flow is assumed to be steady and satisfies $\frac{\partial u}{\partial x} = \frac{\partial v}{\partial x} = v = \frac{\partial T}{\partial x} = 0$ (u and v are the x- and y- components of the velocity $\boldsymbol{u}$). Therefore, both the velocity and distribution functions are only functions of the y-coordinate. Although this type of flow is rather simple, the analyses based on it can provide us some basic theoretical insights of the DSBC.

For the D2Q9 model,[12,17] and the horizontal wall boundary with flow on its upside, Eqs. (15) and (16) can be written explicitly as

$$f_{\alpha=2/3/4} = \frac{6}{\rho_w} f^{\mathrm{eq}}_{\alpha=2/3/4}(\rho_w, \mathrm{u}_w)(f_6 + f_7 + f_8), \tag{17}$$

$$g_{\alpha=2/3/4} = \frac{3}{\rho_w \varepsilon} g^{\mathrm{eq}}_{\alpha=2/3/4}(\rho_w, \mathrm{u}_w, \varepsilon_w)(g_6 + g_7 + g_8). \tag{18}$$

4.1. Velocity Slip Boundary Condition

From Eqs. (1), (3), (4), and (17), on the wall boundary, we obtain the following equations:

$$\bar{f}_0^{j=1} = \frac{4}{9}\rho\left(1 - \frac{3}{2}\frac{u_{j=1}^2}{c^2}\right), \tag{19a}$$

$$\bar{f}_1^{j=1} = \frac{1}{9}\rho\left(1 + 3\frac{u_{j=1}}{c} + \frac{9}{2}\frac{u_{j=1}^2}{c^2} - \frac{3}{2}\frac{u_{j=1}^2}{c^2}\right), \tag{19b}$$

$$\begin{aligned}\bar{f}_2^{j=1} = {} & \frac{\tau_f + 0.5\delta_t}{6\tau_f}\left(1 + 3\frac{U_0}{c} + \frac{9}{2}\frac{U_0^2}{c^2} - \frac{3}{2}\frac{U_0^2}{c^2}\right)(f_6^{j=1} + f_7^{j=1} + f_8^{j=1}) \\ & - \frac{\delta_t}{72\tau_f}\rho\left(1 + 3\frac{u_{j=1}}{c} + \frac{9}{2}\frac{u_{j=1}^2}{c^2} - \frac{3}{2}\frac{u_{j=1}^2}{c^2}\right),\end{aligned} \tag{19c}$$

$$\bar{f}_3^{j=1} = \frac{2(\tau_f + 0.5\delta_t)}{3\tau_f}\left(1 - \frac{3}{2}\frac{U_0^2}{c^2}\right)(f_6^{j=1} + f_7^{j=1} + f_8^{j=1}) - \frac{\delta_t}{18\tau_f}\rho\left(1 - \frac{3}{2}\frac{u_{j=1}^2}{c^2}\right), \tag{19d}$$

$$\bar{f}_4^{j=1} = \frac{\tau_f + 0.5\delta_t}{6\tau_f}\left(1 - 3\frac{U_0}{c} + \frac{9}{2}\frac{U_0^2}{c^2} - \frac{3}{2}\frac{U_0^2}{c^2}\right)(f_6^{j=1} + f_7^{j=1} + f_8^{j=1}) - \frac{\delta_t}{72\tau_f}\rho\left(1 - 3\frac{u_{j=1}}{c} + \frac{9}{2}\frac{u_{j=1}^2}{c^2} - \frac{3}{2}\frac{u_{j=1}^2}{c^2}\right), \tag{19e}$$

$$\bar{f}_5^{j=1} = \frac{1}{9}\rho\left(1 - 3\frac{u_{j=1}}{c} + \frac{9}{2}\frac{u_{j=1}^2}{c^2} - \frac{3}{2}\frac{u_{j=1}^2}{c^2}\right), \tag{19f}$$

$$\bar{f}_6^{j=1} = \frac{\delta_t}{36(\tau_f + 0.5\delta_t)}\rho\left(1 - 3\frac{u_{j=2}}{c} + \frac{9}{2}\frac{u_{j=2}^2}{c^2} - \frac{3}{2}\frac{u_{j=2}^2}{c^2}\right) + \frac{\tau_f - 0.5\delta_t}{\tau_f + 0.5\delta_t}\bar{f}_6^{j=2}, \tag{19g}$$

$$\bar{f}_7^{j=1} = \frac{\delta_t}{9(\tau_f + 0.5\delta_t)}\rho\left(1 - \frac{3}{2}\frac{u_{j=2}^2}{c^2}\right) + \frac{\tau_f - 0.5\delta_t}{\tau_f + 0.5\delta_t}\bar{f}_7^{j=2}, \tag{19h}$$

$$\bar{f}_8^{j=1} = \frac{\delta_t}{36(\tau_f + 0.5\delta_t)}\rho\left(1 + 3\frac{u_{j=2}}{c} + \frac{9}{2}\frac{u_{j=2}^2}{c^2} - \frac{3}{2}\frac{u_{j=2}^2}{c^2}\right) + \frac{\tau_f - 0.5\delta_t}{\tau_f + 0.5\delta_t}\bar{f}_8^{j=2}, \tag{19i}$$

where $j=1$ represents the wall boundary and $j=2$ is its neighboring layer. From Eqs. (19a–i), one can easily prove the normal momentum $\rho v_{j=1}=0$. The tangential momentum $\rho u_{j=1}$ can be written as

$$\rho u_{j=1} = c(\bar{f}_1^{j=1} - \bar{f}_5^{j=1} + \bar{f}_2^{j=1} - \bar{f}_4^{j=1} + \bar{f}_8^{j=1} - \bar{f}_6^{j=1}). \tag{20}$$

Substituting Eqs. (19a–i) into Eq. (20), we can get

$$\rho u_{j=1} = c\left\{\frac{2}{3}\rho\frac{u_{j=1}}{c} + \frac{\tau_f + 0.5\delta_t}{\tau_f}\frac{U_0}{c}(f_6^{j=1} + f_7^{j=1} + f_8^{j=1}) - \frac{\delta_t}{12\tau_f}\frac{\rho u_{j=1}}{c} + \frac{\delta_t}{6(\tau_f + 0.5\delta_t)}\frac{\rho u_{j=2}}{c} + \frac{\tau_f - 0.5\delta_t}{\tau_f + 0.5\delta_t}(\bar{f}_8^{j=2} - \bar{f}_6^{j=2})\right\}. \tag{21}$$

Applying the tangential momentum definition ρu at $j = 2$ in Eq. (21) and noting $\bar{f}_1^{j=2} - \bar{f}_5^{j=2} = \frac{2}{3}\rho\frac{u_{j=2}}{c}$ because of zero gradient flow along x-direction assumed in this analysis, we have

$$\rho u_{j=1} = c\left\{\frac{8\tau_f - \delta_t}{12\tau_f}\rho\frac{u_{j=1}}{c} + \frac{\tau_f + 0.5\delta_t}{6\tau_f}\frac{\rho U_0}{c} + \frac{\tau_f}{3(\tau_f + 0.5\delta_t)}\frac{\rho u_{j=2}}{c} - \frac{\tau_f - 0.5\delta_t}{\tau_f + 0.5\delta_t}(\bar{f}_2^{j=2} - \bar{f}_4^{j=2})\right\}, \tag{22}$$

which further yields

$$\rho u_{j=1} = c\left\{\frac{2}{3}\rho\frac{u_{j=1}}{c} + \frac{\delta_t}{3(\tau_f + 0.5\delta_t)}\frac{\rho U_0}{c} + \frac{\tau_f}{3(\tau_f + 0.5\delta_t)}\frac{\rho u_{j=2}}{c} - \frac{\delta_t}{6(\tau_f + 0.5\delta_t)}\rho\frac{u_{j=1}}{c}\right\}. \tag{23}$$

Through simple algebraic operation for Eq. (23), the slip velocity on the wall can then be obtained

$$U_s = u_{j=1} - U_0 = \frac{\tau_f}{\delta_t}(u_{j=2} - u_{j=1}). \tag{24}$$

Making Taylor series expansion of $u_{j=2}$ to the boundary and dropping the subscript index, and using Eq. (9), we have

$$U_S = u_w - U_0 = Kn\frac{\partial u}{\partial n} + \frac{Kn\delta}{2}\frac{\partial^2 u}{\partial n^2} + \cdots, \tag{25}$$

which is exactly the same as the one given from the high-order velocity slip model[23] if the neighboring layer to the boundary is set at one mean free path of molecules away from the boundary.

4.2. Temperature Jump Boundary Condition

For simplicity, we neglect the effects of the heat dissipation in the following analysis. From Eqs. (2), (3), (5) and (18), on the wall boundary, we obtain the following equations:

$$\bar{g}_0^{j=1} = \frac{4}{9}\rho\varepsilon_{j=1}\left(-\frac{3}{2}\frac{u_{j=1}^2}{c^2}\right), \tag{26a}$$

$$\bar{g}_1^{j=1} = \frac{1}{9}\rho\varepsilon_{j=1}\left(1.5+1.5\frac{u_{j=1}}{c}+\frac{9}{2}\frac{u_{j=1}^2}{c^2}-\frac{3}{2}\frac{u_{j=1}^2}{c^2}\right), \tag{26b}$$

$$\begin{aligned}\bar{g}_2^{j=1} = {} & \frac{\tau_g+0.5\delta_t}{12\tau_g}\frac{\varepsilon_0}{\varepsilon_{j=1}}\left(3+6\frac{U_0}{c}+\frac{9}{2}\frac{U_0^2}{c^2}-\frac{3}{2}\frac{U_0^2}{c^2}\right)\left(g_6^{j=1}+g_7^{j=1}+g_8^{j=1}\right)\\ & -\frac{\delta_t}{72\tau_g}\rho\varepsilon_{j=1}\left(3+6\frac{u_{j=1}}{c}+\frac{9}{2}\frac{u_{j=1}^2}{c^2}-\frac{3}{2}\frac{u_{j=1}^2}{c^2}\right),\end{aligned} \tag{26c}$$

$$\begin{aligned}\bar{g}_3^{j=1} = {} & \frac{\tau_g+0.5\delta_t}{3\tau_g}\frac{\varepsilon_0}{\varepsilon_{j=1}}\left(1.5-\frac{3}{2}\frac{U_0^2}{c^2}\right)\left(g_6^{j=1}+g_7^{j=1}+g_8^{j=1}\right)\\ & -\frac{\delta_t}{18\tau_g}\rho\varepsilon_{j=1}\left(1.5-\frac{3}{2}\frac{u_{j=1}^2}{c^2}\right),\end{aligned} \tag{26d}$$

$$\begin{aligned}\bar{g}_4^{j=1} = {} & \frac{\tau_g+0.5\delta_t}{12\tau_g}\frac{\varepsilon_0}{\varepsilon_{j=1}}\left(3-6\frac{U_0}{c}+\frac{9}{2}\frac{U_0^2}{c^2}-\frac{3}{2}\frac{U_0^2}{c^2}\right)\left(g_6^{j=1}+g_7^{j=1}+g_8^{j=1}\right)\\ & -\frac{\delta_t}{72\tau_g}\rho\varepsilon_{j=1}\left(3-6\frac{u_{j=1}}{c}+\frac{9}{2}\frac{u_{j=1}^2}{c^2}-\frac{3}{2}\frac{u_{j=1}^2}{c^2}\right),\end{aligned} \tag{26e}$$

$$\bar{g}_5^{j=1} = \frac{1}{9}\rho\varepsilon_{j=1}\left(1.5-1.5\frac{u_{j=1}}{c}+\frac{9}{2}\frac{u_{j=1}^2}{c^2}-\frac{3}{2}\frac{u_{j=1}^2}{c^2}\right), \tag{26f}$$

$$\bar{g}_6^{j=1} = \frac{\delta_t}{36(\tau_g + 0.5\delta_t)}\rho\varepsilon_{j=1}\left(3 - 6\frac{u_{j=2}}{c} + \frac{9}{2}\frac{u_{j=2}^2}{c^2} - \frac{3}{2}\frac{u_{j=2}^2}{c^2}\right) + \frac{\tau_g - 0.5\delta_t}{\tau_g + 0.5\delta_t}\bar{g}_6^{j=2}, \tag{26g}$$

$$\bar{g}_7^{j=1} = \frac{\delta_t}{9(\tau_g + 0.5\delta_t)}\rho\varepsilon_{j=1}\left(1.5 - \frac{3}{2}\frac{u_{j=2}^2}{c^2}\right) + \frac{\tau_g - 0.5\delta_t}{\tau_g + 0.5\delta_t}\bar{g}_7^{j=2}, \tag{26h}$$

$$\bar{g}_8^{j=1} = \frac{\delta_t}{36(\tau_g + 0.5\delta_t)}\rho\varepsilon_{j=1}\left(3 + 6\frac{u_{j=2}}{c} + \frac{9}{2}\frac{u_{j=2}^2}{c^2} - \frac{3}{2}\frac{u_{j=2}^2}{c^2}\right) + \frac{\tau_g - 0.5\delta_t}{\tau_g + 0.5\delta_t}\bar{g}_8^{j=2}. \tag{26i}$$

The internal energy $\rho\varepsilon$ on the wall boundary can be written as

$$\rho\varepsilon_{j=1} = \sum_{\alpha=0}^{8}\bar{g}_\alpha^{j=1}. \tag{27}$$

Substituting Eqs. (26a–i) into Eq. (27), we can get

$$\rho\varepsilon_{j=1} = \left\{\frac{1}{3}\rho\varepsilon_{j=1} + \frac{(\tau_g + 0.5\delta_t)}{\tau_g}\frac{\varepsilon_0}{\varepsilon_{j=1}}(g_6^{j=1} + g_7^{j=1} + g_8^{j=1}) - \frac{\delta_t}{6\tau_g}\rho\varepsilon_{j=1} + \frac{\delta_t}{3(\tau_g + 0.5\delta_t)}\rho\varepsilon_{j=2} + \frac{\tau_g - 0.5\delta_t}{\tau_g + 0.5\delta_t}(\bar{g}_6^{j=2} + \bar{g}_7^{j=2} + \bar{g}_8^{j=2})\right\}. \tag{28}$$

Applying the internal energy definition $\rho\varepsilon$ at $j=2$ in Eq. (28) and noting $g_0^{j=2} + g_1^{j=2} + g_5^{j=2} = \frac{1}{3}\rho\varepsilon_{j=2}$, we have

$$\rho\varepsilon_{j=1} = \left\{\frac{1}{3}\rho\varepsilon_{j=1} + \frac{(\tau_g + 0.5\delta_t)}{3\tau_g}\varepsilon_0 - \frac{\delta_t}{6\tau_g}\rho\varepsilon_{j=1} + \frac{2\tau_g}{3(\tau_g + 0.5\delta_t)}\rho\varepsilon_{j=2} - \frac{\tau_g - 0.5\delta_t}{\tau_g + 0.5\delta_t}(\bar{g}_2^{j=2} + \bar{g}_3^{j=2} + \bar{g}_4^{j=2})\right\}, \tag{29}$$

which further yields

$$\rho\varepsilon_{j=1} = \left\{ \frac{1}{3}\rho\varepsilon_{j=1} + \frac{2\delta_t}{3(\tau_g + 0.5\delta_t)}\varepsilon_0 - \frac{\delta_t}{3(\tau_g + 0.5\delta_t)}\rho\varepsilon_{j=1} + \frac{2\tau_g}{3(\tau_g + 0.5\delta_t)}\rho\varepsilon_{j=2} \right\}. \tag{30}$$

Through simple algebraic operation for Eq. (30) and noting $\varepsilon = RT$, the temperature jump on the wall can then be obtained

$$T_s = T_{j=1} - T_0 = \frac{\tau_g}{\delta_t}(T_{j=2} - T_{j=1}). \tag{31}$$

Making Taylor series expansion of $T_{j=2}$ to the boundary and dropping the subscript index, and using Eq. (10), we have

$$T_S = T_w - T_0 = \frac{Kn}{\Pr}\frac{\partial T}{\partial n} + \frac{Kn\delta}{2\Pr}\frac{\partial^2 T}{\partial n^2} + \cdots, \tag{32}$$

which is similar to the one given from the high-order temperature jump model[23] if the neighboring layer to the boundary is set at one mean free path of molecules away from the boundary.

It can be seen from Eqs (25) and (32) that, to get the higher order approximation, the slip velocity and jump temperature depend on both Kn and δ. From the kinetic theory, Kn is related to the viscosity, and usually, δ is taken as the minimum mesh spacing. So, the slip velocity and jump temperature depend on the viscosity and the grid resolution.

5. NUMERICAL SIMULATIONS

In order to validate the lattice BGK model presented above numerically, a 2D thermal Couette flow and a developing thermal microchannel flow are simulated. All simulations are based on the D2Q9 model. All results presented in the following have been tested by grid-independence study.

5.1. 2D Thermal Couette Flow

Considering a thermal Couette flow confined between two plates parallel to the x-axis at $y = \pm H$. The plates are moving oppositely with a constant velocity U_0 and having temperatures T_0 at the lower plate and T_1 at the upper plate, respectively. The major control parameters are the Prandtl number Pr measuring the moment to heat diffusivity and the Eckert number $Ec = U_0^2/c_v(T_1 - T_0)$ (if $T_1 > T_0$) measuring the kinetic to internal

energy. In present work, we set $\Pr = 0.71$ and $U_0 = 0.1$. The DSBC is used on the both plates after the stream process of the particles. Periodic boundary conditions are used at the inlet and outlet. All simulations in this part are based on a 31×31 uniform grid and all results presented are normalized by U_0, T_0 and H, respectively.

Figure 1 shows velocity profiles between two plates at three different grid numbers at $Kn = 0.2$. Obviously, all results are shown to be highly consistent though the grid number changes. However, as shown in Fig. 1, the present model does not capture the expected Knudsen layer (nonlinear distribution) although the Knudsen number is considered in the present model. The reason may be due to the fact that the Knudsen layer is the region with high nonequilibrium, where the high-order hydrodynamics such as stress tensors is dominated and the present model does not consider it sufficiently. Figure 2(a) and (b) shows the normalized temperature profiles of $Kn = 0.05$, 0.1 and 0.3 with $Ec = 10$ and $Ec = 2$, 10 and 20 with

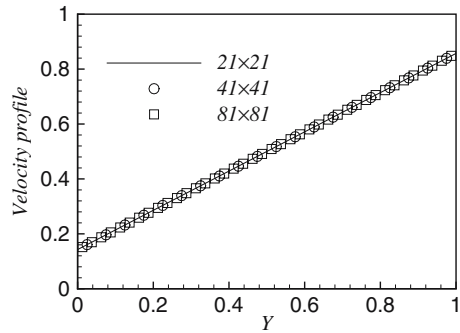

Fig. 1. Velocity profiles between two plates for different grids at $Kn = 0.2$.

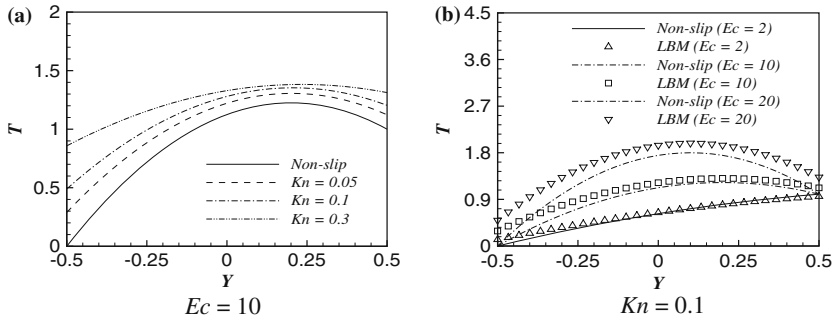

Fig. 2. Normalized temperature profiles between two plates for (a) different Knudsen numbers and (b) different Eckert numbers.

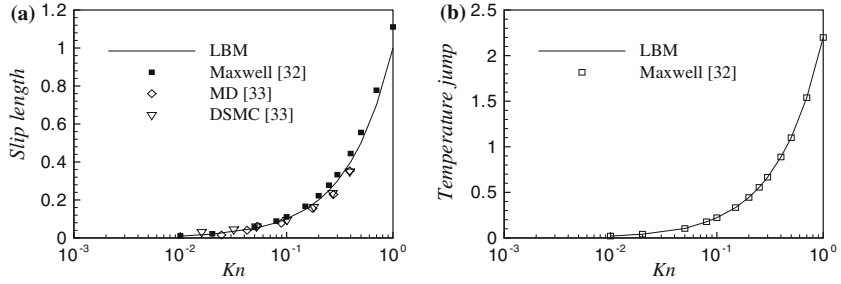

Fig. 3. Variation of the dimensionless (a) slip length and (b) temperature jump with the Knudsen numbers.

$Kn = 0.1$ between the plates, respectively. The Knudsen effects on the viscous heat dissipation behaviors can be observed in Fig. 1(a). As shown in Fig. 2(a) and (b), the temperature profiles between the plates are parabolic and the obvious temperature jumps are found for all Knudsen numbers. Due to rarefaction of the flow, the heat behavior is more demonstrated with the increasing Ec (Fig.2 (b)). The velocity slip and temperature jump can be seen in Fig. 3(a) and (b), which show variations of the dimensionless slip length $\xi = (U_w - U_0)/\dot{\gamma}$ ($\dot{\gamma} = \partial u/\partial y$) and temperature jump $l = (T_w - T_0)/\dot{\theta}$ ($\dot{\theta} = \partial T/\partial Y$)) with the Knudsen numbers in the range of 0.01 to 1. Results obtained by the DSMC, MD and Maxwell theoretical analysis are also included in these figures to see the accuracy of the present model. The DSMC and MD methods have been well established for accurately modelling high-Knudsen-number flows.[28,32] Maxwell theory predicts that the slip length and temperature jump are about $\xi = 1.15Kn$ and $l = 2.26Kn$.[28] As shown in Fig. 3(a) and (b), the present results are in good agreement with those from the Maxwell prediction,[21] the DSMC approach and MD method[32] in the slip flow regime ($Kn \leqslant 0.1$). As Kn increases, the present results lie in between the results of the Maxwell theory and those of the DSMC and MD simulations.

5.2. Thermal Developing Flow in Microchannel

The thermal developing flow in a microchannel is another test case for the present lattice Boltzmann model. Here we consider a flow at $Re = 0.01$, which is confined between two parallel plates with length L and locating at $\pm H/2$ ($L/H = 20$). Initially, the flow is assumed static with constant temperature T_0 and the plates are heated uniformly with a constant temperature T_w ($T_w = 10T_0$). The Prandtl number is fixed as $\Pr = 0.7$. During simulations, a uniform velocity $U_0 = 0.1$ is imposed at the inlet of the

microchannel and the variables at outlet are extrapolated from the interior flow field. The DSBC is used on the plates for the density and internal energy density distribution functions. A nonuniform grid of 201×29 is used and the grid points are clustered near the wall and inlet of the microchannel.

For the thermal developing flow problems in channels, friction, heat and mass transfer are of most interest and they can be measured by the local wall friction coefficient C_f $(= \frac{\mu(\partial u/\partial y)_w}{(1/2)\rho u_b^2})$ and local wall Nusselt number Nu $(= \frac{2H(\partial T/\partial y)_w}{(T_w - T_b)})$. Here u_b and T_b are the bulk velocity and temperature and u is the velocity component in the x-direction. Figure 4 shows the effects of the inlet Kn on the friction coefficients and Nusselt numbers along the channel. As shown in Fig. 4, increasing Kn causes $C_f Re$ and Nu decreased. The entrance region where the flow is developing is larger for higher Kn due to the larger velocity slip caused. Table I compares the values of $C_f Re$ and Nu for different Kn_{in} with those roughly grabbed from the figures presented by Kavehpour *et al.*[33] The first-order analytical prediction of $C_f Re$ by Karniadakis and Beskok[23] is also included for comparison. From Table I, one can see that the present lattice Boltzmann model gives a good prediction of the flow behaviors compared to the works of Kavehpour *et al.*[33] and Karniadakis and Beskok.[23]

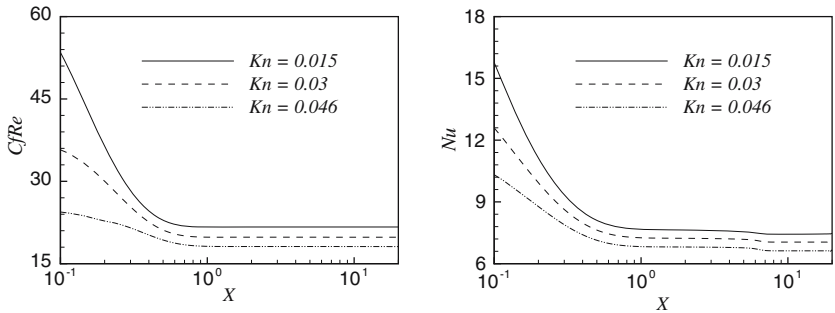

Fig. 4. Effect of Kn_{in} on friction coefficient (left) and Nusselt number (right).

Table I. Comparisons of the Outlet $C_f Re$ and Nu Obtained by Different Methods

Kn_{in}	C_f [23]	C_f [33]	C_f (present)	Nu [33]	Nu (present)
0.015	22.02	21.9	21.69	7.4	7.48
0.03	20.34	20	19.81	7.0	7.07
0.046	18.81	18	18.11	6.6	6.63

6. CONCLUSIONS

A lattice Boltzmann BGK model for simulation of the micro flow and heat transfer has been presented based on the kinetic theory and the TLBM. Following the kinetic theory, the relaxation times in the LBM are linked to the Knudsen number. A diffuse scattering boundary condition for the velocity and temperature at the wall is also derived from the kinetic theory. Theoretical analyses of the DSBC based on the D2Q9 discrete velocity model for a simple 2D plane thermal flow have been presented, and our analytical results are similar to the high-order slip/jump models of Beskok[23] if the neighboring layer to the boundary is set at one mean free path of molecules away from the boundary.

Numerical simulations of the 2D thermal Couette flow with a thermal gradient and the developing thermal flow in a microchannel are carried out and the results are in good agreement with the previous studies. The present studies show that the present method gives a good prediction of the micro fluidic behaviors with thermal effects.

REFERENCES

1. D. B. Tuckerman and R. F. W. Pease, *IEEE Electron. Device Lett.* **EDL-2**:126 (1981).
2. P. Y. Wu and W. A. Little, *Cryogenics* **24**:415 (1984).
3. X. F. Peng, G. P. Peterson, and B. X. Wang, *Experimental Heat Transfer* **7**:265 (1994).
4. C. Yang, D. Li, and J. H. Masliyah, *Int. J. Heat Mass Transfer* **41**:4229 (1998).
5. F. Sharipov and V. Seleznev, *J. Phys. Chem. Ref. Data* **27**:657 (1998).
6. S. K. Loyalka and S. A. Hamoodi, *Phys. Fluids* A **2**:2061 (1990).
7. T. Ohwada, Y. Sone, and K. Aoki, *Phys. Fluids* A **1**:2042 (1989).
8. B. J. Alder and T. E. Waiwright, *J. Chem. Phys*. **27**:1208 (1957).
9. G. Bird, *Molecular Gas Dynamics and the Direct Simulation of Gas Flows* (Oxford Science Publications, 1994).
10. F. Higuera, S. Succi, and R. Benzi, *Europhys. Lett.* **9**:345 (1989).
11. R. Benzi, S. Succi, and M. Vergassola, *Phys. Rep.* **222**:145 (1992).
12. Y. H. Qian, D. d'Humiéres, and P. Lallemand, *Europhys. Lett*. **17**:479 (1992).
13. S. Chen and G. D. Doolen, *Ann. Rev. Fluid Mech*. **30**:329 (1998).
14. H. Chen, S. Kandasamy, S. Orszag, R. Shock, S. Succi, and V. Yakhot, *Science* **301**:633 (2003).
15. P. L. Bhatnagar, E. P. Gross, and M. Krook, *Phys. Rev.* **94**:511 (1954).
16. C. Cercignani, *Mathematical Methods in Kinetic Theory* (Plenum, New York, 1969).
17. X. He, S. Chen, and G. D. Doolen, *J. Comp. Phys.* **146**:282 (1998).
18. S. Chapman and T. Cowling, *Mathematical Theory of Non-uniform Gases*, 3rd edn. (Cambridge University Press, UK, 1970).
19. G. E. Karniadakis and A. Beskok, *Micro Flows: Fundamentals and Simulation* (Springer-Verlag, New York, 2002).
20. C. Shu, Y. T. Chew, and X. D. Niu, *Phys. Rev.* E **64**:045701–1 (2001).
21. C. Shu, X. D. Niu, and Y. T. Chew, *Phys. Rev.* E **65**:036708–1 (2002).
22. Y. T. Chew, C. Shu, and X. D. Niu, *Int. J. Mod. Phys.* C **13**:719 (2002).
23. G. Wannier, *Statistical Physics* (Dover, New York, 1966).

24. X. Nie, G. D. Doolen, and S. Chen, *J. Stat. Phys*. **107**(1/2):279 (2002).
25. C. Y. Lim, C. Shu, X. D. Niu, and Y. T. Chew, *Phys. Fluids* **14**:2299 (2002).
26. S. Succi, *Phys. Rev. Lett*. **89**:64502 (2002).
27. S. Succi, G. Amati, and R. Benzi, C, *J. Stat. Phys.* **8**1(1/2):5 (1995).
28. D. R. Willis, *Phys. Fluids* **5**:127 (1963).
29. J. C. Maxwell, in *The Scientific Papers of James Clerk Maxwell*, Vol. 2, W. D. Niven, ed., (Dover, New York, 1952).
30. R. Gatignol, *Phys. Fluids* **20**:2022 (1977).
31. S. Ansumali and I. V. Karlin, *Phys. Rev.* E **66**:026311–1 (2002).
32. D. L. Morris, L. Hannon, and A. L. Garcia, *Phys. Rev.* A **46**:5279 (1992).
33. H. P. Kavehpour, M. Faghri, and Y. Asako, *Numer. Heat Transfer*, Part A **32**:677 (1997).